Biochemical and Biophysical Research Communications 410 (2011) 134–139

Contents lists available at ScienceDirect

Biochemical and Biophysical Research Communications

journal homepage: www.elsevier.com/locate/ybbrc

Selective cell-surface labeling of the molecular motor protein prestin

Ryan M. McGuire [a], Jonathan J. Silberg [a,b,*], Fred A. Pereira [a,c], Robert M. Raphael [a,*]

[a] Department of Bioengineering, Rice University, Houston, TX 77251, USA
[b] Department of Biochemistry and Cell Biology, Rice University, Houston, TX 77251, USA
[c] Huffington Center on Aging, Department of Molecular and Cellular Biology, Baylor College of Medicine, Houston, TX 77030, USA

ARTICLE INFO

Article history:
Received 12 May 2011
Available online 27 May 2011

Keywords:
Biotinylation
Charge transfer
Electrophysiology
Membrane protein
Molecular motor
Prestin
Protein engineering

ABSTRACT

Prestin, a multipass transmembrane protein whose N- and C-termini are localized to the cytoplasm, must be trafficked to the plasma membrane to fulfill its cellular function as a molecular motor. One challenge in studying prestin sequence-function relationships within living cells is separating the effects of amino acid substitutions on prestin trafficking, plasma membrane localization and function. To develop an approach for directly assessing prestin levels at the plasma membrane, we have investigated whether fusion of prestin to a single pass transmembrane protein results in a functional fusion protein with a surface-exposed N-terminal tag that can be detected in living cells. We find that fusion of the biotin-acceptor peptide (BAP) and transmembrane domain of the platelet-derived growth factor receptor (PDGFR) to the N-terminus of prestin-GFP yields a membrane protein that can be metabolically-labeled with biotin, trafficked to the plasma membrane, and selectively detected at the plasma membrane using fluorescently-tagged streptavidin. Furthermore, we show that the addition of a surface detectable tag and a single-pass transmembrane domain to prestin does not disrupt its voltage-sensitive activity.

1. Introduction

In response to changes in transmembrane potential, mammalian sensory outer hair cells (OHCs) change length [1–3]. This motion enhances sound-induced vibrations within the cochlea and improves hearing sensitivity [4]. The transmembrane protein prestin is critical for this signal amplification process [5]. Prestin is a molecular motor within the plasma membrane that responds to changes in transmembrane potential, and the electrical activity of prestin is tightly coupled to changes in the length of OHCs [6,7]. The physiological role of prestin's electromechanical coupling (molecular piezoelectricity) function in hearing has been clearly delineated [8,9]. Prestin responds to cellular depolarization by reducing cell length, whereas prestin increases cell length when cells become hyperpolarized. Currently, the molecular mechanism of voltage-to-length conversion within this multipass transmembrane protein is not understood.

In contrast to other widely studied molecular motors (e.g., myosin, kinesin, and dynein), prestin does not require ATP or calcium for motor function [3,10]. Prestin belongs to a family of anionic membrane transport proteins, solute carrier family 26 (SLC26), for which little structural information is available. Like all membrane proteins, prestin function requires proper insertion into the plasma membrane. This latter property makes prestin challenging to study upon heterologous expression in cultured cells, since transiently transfected cells exhibit heterogeneity in both the level of prestin expressed and the amount of prestin trafficked to the plasma membrane [11,12]. In addition, mutation of prestin can alter these properties as well as electromechanical coupling, making it difficult to interpret the effects of amino acid substitutions or deletions [13]. Since mutagenesis coupled with functional analysis is widely used to study prestin [11,14–21], an ability to selectively identify, and potentially quantify, the membrane-localized fraction would greatly enhance the biochemical and biophysical information gleaned from these studies.

To establish a strategy for studying the function of membrane-localized prestin, we investigated whether prestin could be metabolically tagged in living cells with biotin, a vitamin that binds with high affinity [22,23] to streptavidin-conjugated fluorophores. The lack of endogenous surface biotinylation in mammalian cells [24,25], and the impermeability of cell membranes to streptavidin conjugates makes this strategy compatible with selective labeling and purification of surface expressed membrane proteins. We based our reporter construct on the most extensively studied endogenously biotinylated protein, the 1.3 S subunit of *Propionibacterium shermanii* transcarboxylase (commonly called PSTCD) [26]. The biotin acceptor peptide (BAP) sequence from PSTCD has been fused to the C-terminus of multiple cytoplasmic enzymes and demonstrated to undergo in vivo metabolic biotinylation in both bacteria and yeast [27]. Parrot and Barry extended this technology to metazoans [28], and they demonstrated that both secreted and simple, single-pass integral membrane proteins can

* Corresponding authors. Address: Department of Bioengineering, Rice University, 6500 Main Street, Houston, TX 77030, USA
E-mail addresses: joff@rice.edu (J.J. Silberg), rraphael@rice.edu (R.M. Raphael).

0006-291X/$ - see front matter © 2011 Elsevier Inc. All rights reserved.
doi:10.1016/j.bbrc.2011.05.121

be biotinylated [29]. One of their constructs, BAP fused to the N-terminus of the platelet-derived growth factor receptor (PDGFR) transmembrane domain, was used to introduce streptavidin conjugated contrast agents to the surface of tumor cells and enhance magnetic resonance imaging (MRI) [30]. Herein, we demonstrate the first use of BAP-PDGFR for extracellular biotinylation of a multi-pass transmembrane protein.

2. Materials and methods

2.1. Plasmid construction

The 736 bp BAP-PDGFR reporter gene was synthesized from a 24 primer set, composed primarily of 50 bp oligonucleotides, designed using DNAWorks (Helix Systems, NIH) and the PCR-based synthesis methods of Hoover and Lubkowski [31].The gene includes a 5′ NheI restriction site and a 3′ HindIII restriction site, and it encodes the murine Ig κ-chain leader sequence, the hemagglutinin A (HA) epitope tag, a biotin acceptor peptide (BAP), the transmembrane domain from platelet-derived growth factor receptor (PDGFR), and a 19 amino acid cytoplasmic linker region. Fig. 1A illustrates the protein fusion expressed by this construct. The BAP coding sequence was derived from base pairs 1–390 of the PinPoint Xa vector (Promega, Madison, WI). The murine Ig κ-chain leader sequence, which targets the fusion to the secretory pathway [32], and the PDGFR transmembrane domain, which ensures exoplasmic display of BAP [33], were isolated from base pairs 737–799 and 907–1053 (respectively) of the pDisplay vector (Invitrogen, Carlsbad, CA). All nucleotide segments were codon

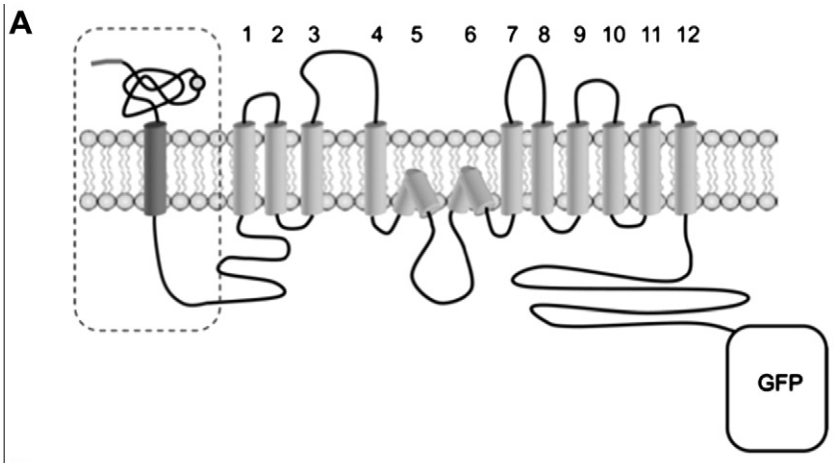

B

METDTLLLWV LLLWVPGSTG DYPYDVPDYA AAAAMKLKVT VNGTAYDVDV
DVDKSHENPM GTILFGGGTG GAPAPAAGGA GAGKAGEGEI PAPLAGTVSK
ILVKEGDTVK AGQTVLVLEA MKMETEINAP TDGKVEKVLV KERDAVQGGQ
GLIKIGDLEL IEGRAAAAAV GQDTQEVIVV PHSLPFKVVV ISAILALVVL
TIISLIILIM LWQKKPRGSA GSAGSAGSAD DDDKGSAKAS NSTMDHAEEN
EIPVATQKYH VERPIFSHPV LQERLHVKDK VSESIGDKLK QAFTCTPKKI
RNIIYMFLPI TKWLPAYKFK EYVLGDLVSG ISTGVLQLPQ GLAFAMLAAV
PPVFGLYSSF YPVIMYCFFG TSRHISIGPF AVISLMIGGV AVRLVPDDIV
IPGGVNATNG TEARDALRVK VAMSVTLLSG IIQFCLGVCR FGFVAIYLTE
PLVRGFTTAA AVHVFTSMLK YLFGVKTKRY SGIFSVVYST VAVLQNVKNL
NVCSLGVGLM VFGLLLGGKE FNERFKEKLP APIPLEFFAV VMGTGISAGF
NLHESYSVDV VGTLPLGLLP PANPDTSLFH LVYVDAIAIA IVGFSVTISM
AKTLANKHGY QVDGNQELIA LGICNSIGSL FQTFSISCSL SRSLVQEGTG
GKTQLAGCLA SLMILLVILA TGFLFESLPQ AVLSAIVIVN LKGMFMQFSD
LPFFWRTSKI ELTIWLTTFV SSLFLGLDYG LITAVIIALL TVIYRTQSPS
YKVLGQLPDT DVYIDIDAYE EVKEIPGIKI FQINAPIYYA NSDLYSNALK
RKTGVNPALI MGARRKAMRK YAKEVGNANI ANAAVVKVDG EVDGENATKP
EEEDDEVKYP PIVIKTTFPE ELQRFMPQTE NVHTIILDFT QVNFIDSVGV
KTLAVMVKEY GDVGIYVYLA GCSPQVVNDL TRNRFFENPA LKELLFHSIH
DAVLGSHVRE AMAEQEASAP PPQDDMEPNA TPTTPEARDP PVAT*MVSKGE*
ELFTGVVPIL VELDGDVNGH KFSVSGEGEG DATYGKLTLK FICTTGKLPV
PWPTLVTTLT YGVQCFSRYP DHMKQHDFFK SAMPEGYVQE RTIFFKDDGN
YKTRAEVKFE GDTLVNRIEL KGIDFKEDGN ILGHKLEYNY NSHNVYIMAD
KQKNGIKVNF KIRHNIEDGS VQLADHYQQN TPIGDGPVLL PDNHYLSTQS
KLSKDPNEKR DHMVLLEFVT AAGITLGMDE LYK

Fig. 1. Predicted BAP-prestin-GFP fusion protein topology .A, The biotin acceptor peptide (BAP) was fused to the exoplasmic face of the platelet-derived growth factor receptor (PDGFR) transmembrane domain and attached to a 20 amino acid cytoplasmic linker. This engineered reporter gene and the 12-pass motor protein prestin were cloned to the pEGFP-N1 plasmid (Clontech) to form a fusion (BAP-prestin-GFP) with a convenient external binding moiety. The protein segment from the BAP-PDGFR reporter gene is shown in dashed outline and the transmembrane helices of the prestin-GFP fusion are numbered. BAP can be cleaved from PDGFR by Factor Xa protease and prestin can be liberated from PDGFR by severing the cytoplasmic linker with Enterokinase. B, Translated sequence of BAP-prestin-GFP. The BAP-PDGFR reporter encompasses amino acids 1-237 (bold), prestin 244-987 (gray), and GFP 995-1233 (italics). The BAP-PDGFR reporter contains a leader sequence (amino acids 1–21), hemagluinin tag (22–30), BAP (35–164), PDGFR transmembrane domain (169–216), and cytoplasmic linker (218–237). Biotinylation occurs at Lys 122 (box). The proteolytic cleavage sites (underlined) allow cleavage of the fusion following residue 164 or 234 by Factor Xa or Enterokinase, respectively. GFP contains A207 K (residue 1201 of overall fusion) modification to prevent formation of non-obligate oligomers.

optimized from their original sources using a human codon frequency table [31].

The pEGFP-N1 vector (Clontech, Palo Alto, CA), which served as a backbone for subsequent cloning, was modified through Quikchange mutagenesis to include a point mutation within GFP. This mutation (denoted A206 K in the literature) is located at residue 207 of the Clontech vector (due to an insertion that enhances mammalian translation efficiency) and prevents non-specific interaction of the fusion proteins [34,35]. The synthesized BAP-PDGFR gene fusion was digested and inserted into the NheI and HindIII sites of the pEGFP-N1 plasmid. Gerbil prestin (AF230376) was isolated (EcoRI and BamHI) from a previously described prestin-GFP fusion [36] and inserted downstream and in-frame with the BAP-PDGFR gene fusion. The resulting construct is referred to as BAP-prestin-GFP and the translated fusion protein sequence is shown in Fig. 1B. The entire fusion was sequenced verified using an eight-primer set (Baylor Sequencing Core, Houston, TX). Prestin-GFP containing the A206 K mutation was used for control activity (nonlinear capacitance) measurements. The pSec-BirA vector [29], which expresses *E. coli* biotin ligase (BirA) needed to biotinylate BAP-prestin-GFP was provided as a generous gift from Dr. Michael Barry.

2.2. Plasmid expression and cell culture

HEK293 cells were grown in T75 flasks and 6-well plates containing DMEM supplemented with 10% BCS (Invitrogen, Carlsbad, CA), 1% penicillin–streptomycin, 14.3 mM HEPES, 16.1 mM NaHCO3, and 10 mg/L (41 μM) d-Biotin (Sigma–Aldrich, St. Louis, MO). Cells were transfected with prestin-GFP, or co-transfected with BAP-prestin-GFP and pSec-BirA plasmids, using 2 μg of each plasmid DNA and 3 μL/plamid Fugene 6 transfection reagent (Roche, Indianapolis, IN) according to manufacturer's directions. For electrophysiology and imaging studies, cells were trypsinized and replated onto #1.5 coverslips or MatTek dishes (MatTek Corp., Ashland, MA) 8–12 h after transfection and then evaluated 48–72 h post-transfection.

2.3. Confocal imaging

Biotinylation of BAP and localization of the BAP-prestin-GFP fusion to the membrane were verified using confocal microscopy 72 h post-transfection. Transfected HEKs were incubated with 5 μg/mL Alexa-633 conjugated streptavidin (Invitrogen, Carlsbad, CA) for 20 min at room temperature. Cells were washed with PBS and imaging was performed on an LSM 510 microscope (Zeiss, Thornwood, New York). GFP and the Alexa-633 conjugated streptavidin (SA-Alexa 633) were excited with 488 nm Argon laser light and 633 nm HeNe laser light, respectively. Using a secondary dichotic and separate band pass filters for each channel, GFP fluorescence was collected between 500 and 530 nm and SA-Alexa 633 fluorescence was collected between 650 and 710 nm. The pinhole for both channels was adjusted to produce an optical slice less than 13 μm (2.9 and 2.1 Airy units for the GFP and SA-Alexa 633 channels, respectively). All imaging was performed using a 63X, 1.4NA objective lens.

2.4. Electrophysiology

Kimax-51 capillary tubes (1.5/0.8 mm OD/ID) were heated on a P-97 puller (Sutter, Novato, CA) to form fine tip micropipettes. The micropipettes were filled with pipette blocking solution (130 mM CsCl, 2 mM MgCl2, 10 mM EGTA, 10 mM HEPES) and threaded onto a Ag^+/AgCl electrode. Coverslips seeded at low cell density formed the base of a patch clamp chamber in which the cells were bathed in extracellular blocking solution (99 mM NaCl, 20 mM TEA-Cl, 2 mM CoCl2, 1.47 mM MgCl2, 1 mM CaCl2, 10 mM HEPES), and an agar bridge provided electrical continuity with the reference bath containing a Ag^+/AgCl reference electrode and pipette blocking solution. Blocking solutions [16] were titrated to pH 7.3 and dextrose added to obtain 300 3 mOsm (Osmette A; Precision Systems, Natick, MA). Patch pipettes produced 2–4 MΩ resistance in open-bath and placement was controlled using a Burleigh PCS-6200Micromanipulator (EXFO Life Sciences, Rochester, NY). On-cell seals in excess of 1 GΩ were obtained from healthy, single cells showing strong GFP fluorescence 48 h post-transfection. Pipette capacitance was compensated, the cell membrane ruptured to establish whole-cell mode, and only cells with series resistance less than 10 MΩ and membrane resistance in excess of 1 GΩ retained for analysis. We apply an 800 Hz, 10 mV sine wave and measure the current response as DC holding potential is stepped from −140 to +140 mV in 2 mV increments (HEKA EPC 10 Plus Amplifier with 18-bit DAC). Using a software-based phase-sensitive detector, implemented in Patchmaster software (HEKA, Mahone Bay, NS), we determine the real and imaginary components of the admittance (the complex current response scaled by the command voltage) and calculate membrane capacitance (Cm) and membrane resistance (Rm) [37]. At each DC potential four complete sinusoidal voltage cycles occur and discrete capacitance values are calculated from the latter three. Capacitance versus voltage (DC holding potential) traces are acquired for each cell and fit to the first derivative of the two-state Boltzmann function (Eq. 1) using MATLAB (MathWorks, Natick, MA).

$$C_m = \frac{Q_{\max}\left(\frac{ze}{KT}\right)}{\exp\left[\left(\frac{ze}{KT}\right)(V - V_{1/2})\right]\left(1 + \exp\left[-(V - V_{1/2})\left(\frac{ze}{KT}\right)\right]\right)^2} + C_{\text{lin}} \qquad (1)$$

$Q_{\max}$ is the maximum nonlinear charge movement provided by prestin. $V_{1/2}$ is the voltage at the peak of the capacitance versus holding potential curve. z is the valence of charge movement by prestin and inversely proportional to the width of the NLC curve. Boltzmann's constant k, absolute temperature T, and the charge carried by an electron e, are all constant values. Since variation in cell size causes differences in the maximal charge transfer ($Q_{\max}$), the charge movement is normalized to C_{lin}, and computed on a cell-by-cell basis. This quantity, designated as charge density, has units of fC/pF [38]. Representative NLC curves are reconstructed from mean $Q_{\max}$, $V_{1/2}$ and z obtained from BAP-prestin-GFP or prestin-GFP expressing cells, and each result is normalized to maximal nonlinear capacitance ($Q_{\max}$ze/4kT) of the corresponding group.

3. Results

3.1. Rationale for protein design

Established biotinylation techniques [39,40] are not suitable for detecting prestin localized to the plasma membrane, since the N- and C-termini of prestin are both intracellular [41]. This precludes use of direct BAP fusions to achieve extracellular labeling. Moreover, the predicted 12 transmembrane helices [16] of prestin are thought to be tightly packed [19], with high conservation of the entire transmembrane domain region among the eutherian clade [42]. This suggests that the insertion of BAP into a predicted surface exposed loop could adversely affect prestin folding and function. To provide an externally accessible biotinylation site without altering the primary sequence of the prestin hydrophobic core, we fused the BAP-PDGFR reporter to the N-terminus of prestin. Additionally, GFP was fused to the C-terminus of prestin to assay successful transfection and visualize intracellular protein localization. Fig. 1A shows the predicted topology of the resultant BAP-prestin-GFP fusion protein.

3.2. Fluorescence imaging

We found that BAP-prestin-GFP is biotinylated and inserts into the plasma membrane, when co-expressed in human embryonic kidney (HEK) cells with the *E. coli* biotin ligase, BirA. Confocal imaging shows that a streptavidin (SA) conjugated fluorophore (SA-Alexa 633) cannot permeate the cell membrane and therefore only labels the membrane-localized fraction of BAP-prestin-GFP in live cells (Fig. 2A). In contrast, BAP-prestin-GFP is not biotinylated in the absence of BirA (data not shown). To establish if BAP-prestin-GFP is metabolically labeled with biotin, we removed pixels with low fluorescent intensity values (the lower 5% or 35% for GFP and SA-Alexa 633, respectively) and then visualized the remaining colocalized signal (pixels with non-zero fluorescent values in each channel). We found that nearly all the SA-Alexa 633 fluorescence coincided with GFP fluorescence (Fig. 2B), indicating that the biotinylated BAP-prestin-GFP is properly trafficked and membrane localized.

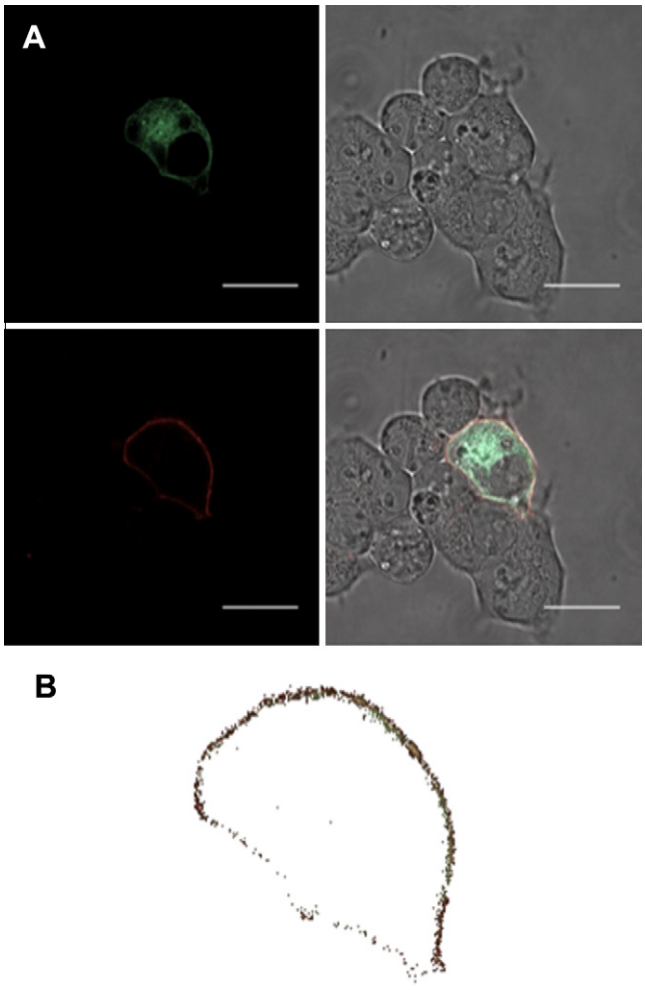

Fig. 2. BAP-prestin-GFP localizes to the cell membrane. A, Brightfield, GFP, SA-Alexa 633, and overlay images (counter-clockwise from upper right) for HEK cells co-transfected with pSec-BirA and BAP-prestin-GFP plasmid DNA. The streptavidin conjugated dye selectively labels the membrane localized fraction of BAP-prestin-GFP and does not non-specifically interact with untransfected HEKs. Scale bar 20 μm. B, After thresholding to remove low intensity pixels, an overlay of the remaining colocalized signal demonstrates efficient biotinylation of BAP-prestin-GFP. 92% of pixels with SA-Alexa 633 fluorescence also have GFP signal, and these are displayed in panel B. Precise one-to-one correspondence was not observed due to slight non-specific background staining and photomultiplier tube (PMT) detector noise.

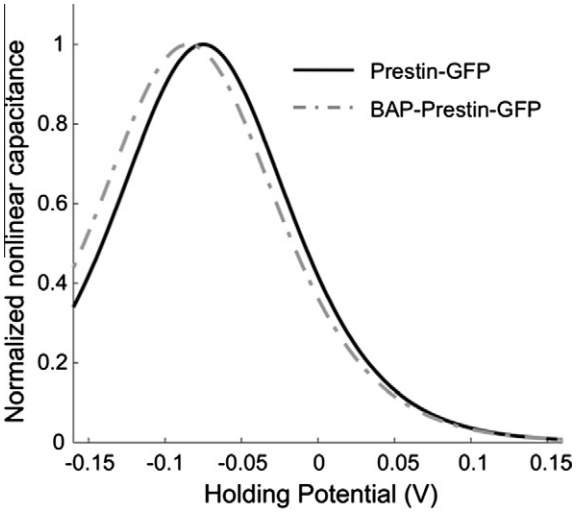

Fig. 3. BAP-prestin-GFP retains activity. NLC curves constructed from mean $V_{1/2}$, z, and Q_{max} (see experimental section) are normalized to the peak capacitance of each group. BAP-prestin-GFP shows normal $V_{1/2}$ and z, and maintains an ability to move charge despite reduction in charge density (Q_{max}/C_{lin}) compared to prestin-GFP ($p < 0.05$). BAP-prestin-GFP ($n = 8$): $V_{1/2}$ −84.8 ± 3.7 mV, z 0.66 ± 0.03, Q_{max}/C_{lin} 3.15 ± 0.29fC/pF. Prestin-GFP ($n = 12$): $V_{1/2}$ −75.1 ± 5.1 mV, z 0.68 ± 0.01, Q_{max}/C_{lin} 18.01 ± 2.87fC/pF. All values are mean ± SE.

3.3. Patch-clamp analysis of prestin function

We next investigated whether the BAP-prestin-GFP fusion retains prestin function. The ability of prestin to move charge within the membrane is tightly coupled to its motor function and has been established as a benchmark for prestin activity [43,44]. We used the whole-cell patch clamp technique to control the voltage across the cell membrane and assayed transmembrane charge movement. In the absence of prestin, HEK cells show uniform, linear capacitance that is proportional to the size of the cell due to the dielectric properties of the plasma membrane [45]. When functional prestin is present in the plasma membrane, a nonlinear, bell-shaped capacitance versus voltage curve is detected [46]. This charge movement, analogous to the gating current in ion channels, is commonly described as nonlinear capacitance (NLC) and thought to result in part from a voltage-induced conformational change in prestin. Fig. 3 shows NLC plots for BAP-prestin-GFP and prestin-GFP without the extra transmembrane domain and BAP reporter. These NLC plots were constructed from mean fit parameters (see experimental section for details) and therefore only display the average increase in capacitance (prestin-associated charge movement) above the linear capacitance (membrane surface area). BAP-prestin-GFP clearly is functional, since it shows bell-shaped NLC comparable to wild-type prestin lacking a BAP fusion. With BAP-prestin-GFP, the voltage at peak capacitance ($V_{1/2}$) and valence of charge movement (z) are indistinguishable from prestin-GFP. This confirms that the operating range and voltage sensitivity of prestin activity were not impacted by the BAP-PDGFR reporter fusion. There was a reduced charge density (Q_{max}/C_{lin}) with the N-terminal fusion that might reflect a lower trafficking and reduced surface expression compared to the unmodified prestin-GFP. This reduced surface expression will be advantageous for future single molecule tracking experiments.

4. Discussion

The findings described herein provide the first evidence that a BAP-PDGFR reporter can be used with a multi-pass transmembrane protein for in vivo biotinylation and subsequent detection. This approach is particularly useful for identifying the mem-

brane-localized fraction of a target protein or introducing a fluorescent label when commercially available antibodies are insufficient. For prestin, live cell labeling is not currently possible in the absence of BAP-PDGFR using simple affinity tags (e.g., HA, FLAG, or myc tags) that are recognized by commercial antibodies. Intracellular tags have been used as N- or C-termini fusions to detect prestin within fixed, membrane-permeabilized samples. For cell surface detection of prestin, these tags have not been introduced within a surface-exposed region of prestin, due the intracellular localization of prestin's N- and C-termini and because all our attempted insertions have proven to be detrimental to prestin trafficking and function. Furthermore, it remains challenging to develop antibodies directed at a surface-exposed region of prestin for live cell imaging, since extracellularly available epitopes of prestin are poorly defined and of low antigenicity.

Our findings provide direct evidence that biotinylated BAP-prestin-GFP localizes to the plasma membrane and is functional. While biotinylation was achieved metabolically by coexpressing BirA and BAP-prestin-GFP, this post-translational modification could be achieved through the addition of BirA and biotin to tissue culture cells expressing BAP-prestin-GFP. This latter approach may prove to be more efficient, since the amount of BirA and biotin can be easily varied in the growth medium to maximize labeling efficiency. The results described herein show that biotinylated BAP-prestin-GFP will be useful for future biophysical studies. This construct will enhance studies examining the relationship between changes in prestin sequence and function. In its current form, this reporter system will be useful for deconvoluting the effects of mutations on protein expression, translocation, and function. Furthermore, this system can be used to label membrane-localized prestin in live cells with fluorescent probes having larger molar absorptivity (extinction coefficient) [47] and higher quantum yield [48] than intrinsically fluorescent proteins. These brighter fluorophores are expected to enable quantitative fluorescent microscopy and single molecule tracking in future studies of prestin. In addition, this general approach is expected to be compatible with cell-surface labeling of other multi-pass transmembrane proteins, such as prestin homologs in the SLC26 protein family.

Acknowledgments

The authors thank Shirley Liu, Peter Nguyen, Crystal Stanworth, and Peng Zhai for technical support, and Dr. Michael Barry of the Mayo Clinic for donating the pSec-BirA vector. This work was supported by a Hamill Foundation grant (R.M.R. and J.J.S.), a Robert A. Welch Foundation grant C-1614 (J.J.S.), and through NIH-NIDCD R21 DC008134 (R.M.R & F.A.P), R01 DC009622 (R.M.R & F.A.P) and-NSF Career BES 044379 (R.M.R).

References

[1] W.E. Brownell, C.R. Bader, D. Bertrand, Y. De Ribaupierre, Evoked mechanical responses of isolated cochlear outer hair cells, Science 227 (1985) 194–196.
[2] J.F. Ashmore, A fast motile response in guinea-pig outer hair cells: the cellular basis of the cochlear amplifier, J. Physiol. 388 (1987) 323–347.
[3] B. Kachar, W.E. Brownell, R. Altschuler, J. Fex, Electrokinetic shape changes of cochlear outer hair cells, Nature 322 (1986) 365–368.
[4] L. Robles, M.A. Ruggero, Mechanics of the mammalian cochlea, Physiol. Rev. 81 (2001) 1305–1352.
[5] J. Zheng, W. Shen, D.Z. He, K.B. Long, L.D. Madison, P. Dallos, Prestin is the motor protein of cochlear outer hair cells, Nature 405 (2000) 149–155.
[6] D.Z. He, J. Zheng, F. Kalinec, S. Kakehata, J. Santos-Sacchi, Tuning in to the amazing outer hair cell: membrane wizardry with a twist and shout, J. Membr. Biol. 209 (2006) 119–134.
[7] A.A. Spector, N. Deo, K. Grosh, J.T. Ratnanather, R.M. Raphael, Electromechanical models of the outer hair cell composite membrane, J. Membr. Biol. 209 (2006) 135–152.
[8] M.C. Liberman, J. Gao, D.Z. He, X. Wu, S. Jia, J. Zuo, Prestin is required for electromotility of the outer hair cell and for the cochlear amplifier, Nature 419 (2002) 300–304.
[9] P. Dallos, X. Wu, M.A. Cheatham, J. Gao, J. Zheng, C.T. Anderson, S. Jia, X. Wang, W.H. Cheng, S. Sengupta, D.Z. He, J. Zuo, Prestin-based outer hair cell motility is necessary for mammalian cochlear amplification, Neuron 58 (2008) 333–339.
[10] M.C. Holley, J.F. Ashmore, On the mechanism of a high-frequency force generator in outer hair cells isolated from the guinea pig cochlea, Proc. R. Soc. Lond. B Biol. Sci. 232 (1988) 413–429.
[11] R.M. McGuire, H. Liu, F.A. Pereira, R.M. Raphael, Cysteine mutagenesis reveals transmembrane residues associated with charge translocation in prestin, J. Biol. Chem. 285 (2010) 3103–3113.
[12] L. Rajagopalan, L.E. Organ-Darling, H. Liu, A.L. Davidson, R.M. Raphael, W.E. Brownell, F.A. Pereira, Glycosylation regulates prestin cellular activity, J. Assoc. Res. Otolaryngol. 11 (2010) 39–51.
[13] P. Dallos, J. Zheng, M.A. Cheatham, Prestin and the cochlear amplifier, J. Physiol. 576 (2006) 37–42.
[14] D. Oliver, D.Z. He, N. Klocker, J. Ludwig, U. Schulte, S. Waldegger, J.P. Ruppersberg, P. Dallos, B. Fakler, Intracellular anions as the voltage sensor of prestin, the outer hair cell motor protein, Science 292 (2001) 2340–2343.
[15] K. Matsuda, J. Zheng, G.G. Du, N. Klocker, L.D. Madison, P. Dallos, N-linked glycosylation sites of the motor protein prestin: effects on membrane targeting and electrophysiological function, J. Neurochem. 89 (2004) 928–938.
[16] L. Deak, J. Zheng, A. Orem, G.G. Du, S. Aguinaga, K. Matsuda, P. Dallos, Effects of cyclic nucleotides on the function of prestin, J. Physiol. 563 (2005) 483–496.
[17] J. Zheng, G.G. Du, K. Matsuda, A. Orem, S. Aguinaga, L. Deak, E. Navarrete, L.D. Madison, P. Dallos, The C-terminus of prestin influences nonlinear capacitance and plasma membrane targeting, J. Cell Sci. 118 (2005) 2987–2996.
[18] D. Navaratnam, J.P. Bai, H. Samaranayake, J. Santos-Sacchi, N-terminal-mediated homomultimerization of prestin, the outer hair cell motor protein, Biophys. J. 89 (2005) 3345–3352.
[19] L. Rajagopalan, N. Patel, S. Madabushi, J.A. Goddard, V. Anjan, F. Lin, C. Shope, B. Farrell, O. Lichtarge, A.L. Davidson, W.E. Brownell, F.A. Pereira, Essential helix interactions in the anion transporter domain of prestin revealed by evolutionary trace analysis, J. Neurosci. 26 (2006) 12727–12734.
[20] S. Kumano, X. Tan, D.Z. He, K. Iida, M. Murakoshi, H. Wada, Mutation-induced reinforcement of prestin-expressing cells, Biochem. Biophys. Res. Commun. 389 (2009) 569–574.
[21] T. Toth, L. Deak, F. Fazakas, J. Zheng, L. Muszbek, I. Sziklai, A new mutation in the human pres gene and its effect on prestin function, Int. J. Mol. Med. 20 (2007) 545–550.
[22] U. Piran, W.J. Riordan, Dissociation rate constant of the biotin-streptavidin complex, J. Immunol. Methods 133 (1990) 141–143.
[23] N.M. Green, Avidin. Adv Protein Chem 29 (1975) 85–133.
[24] B.H. Robinson, J. Oei, M. Saunders, R. Gravel, [3H]biotin-labeled proteins in cultured human skin fibroblasts from patients with pyruvate carboxylase deficiency, J. Biol. Chem. 258 (1983) 6660–6664.
[25] C.S. Chandler, F.J. Ballard, Regulation of the breakdown rates of biotin-containing proteins in Swiss 3T3–L1 cells, Biochem. J. 251 (1988) 749–755.
[26] D. Samols, C.G. Thornton, V.L. Murtif, G.K. Kumar, F.C. Haase, H.G. Wood, Evolutionary conservation among biotin enzymes, J. Biol. Chem. 263 (1988) 6461–6464.
[27] J.E. Cronan Jr., Biotination of proteins in vivo. A post-translational modification to label, purify, and study proteins, J. Biol. Chem. 265 (1990) 10327–10333.
[28] M.B. Parrott, M.A. Barry, Metabolic biotinylation of recombinant proteins in mammalian cells and in mice, Mol. Ther. 1 (2000) 96–104.
[29] M.B. Parrott, M.A. Barry, Metabolic biotinylation of secreted and cell surface proteins from mammalian cells, Biochem. Biophys. Res. Commun. 281 (2001) 993–1000.
[30] B.A. Tannous, J. Grimm, K.F. Perry, J.W. Chen, R. Weissleder, X.O. Breakefield, Metabolic biotinylation of cell surface receptors for in vivo imaging, Nat. Methods 3 (2006) 391–396.
[31] D.M. Hoover, J. Lubkowski, DNAWorks: an automated method for designing oligonucleotides for PCR-based gene synthesis, Nucleic Acids Res. 30 (2002) e43.
[32] M.J. Coloma, A. Hastings, L.A. Wims, S.L. Morrison, Novel vectors for the expression of antibody molecules using variable regions generated by polymerase chain reaction, J. Immunol. Methods 152 (1992) 89–104.
[33] R.G. Gronwald, F.J. Grant, B.A. Haldeman, C.E. Hart, P.J. O'Hara, F.S. Hagen, R. Ross, D.F. Bowen-Pope, M.J. Murray, Cloning and expression of a cDNA coding for the human platelet-derived growth factor receptor: evidence for more than one receptor class, Proc. Natl. Acad. Sci. USA 85 (1988) 3435–3439.
[34] R.Y. Tsien, The green fluorescent protein, Annu. Rev. Biochem. 67 (1998) 509–544.
[35] D.A. Zacharias, Sticky caveats in an otherwise glowing report: oligomerizing fluorescent proteins and their use in cell biology. Sci STKE 2002 (2002) PE23.
[36] J.N. Greeson, L.E. Organ, F.A. Pereira, R.M. Raphael, Assessment of prestin self-association using fluorescence resonance energy transfer, Brain Res. 1091 (2006) 140–150.
[37] M. Lindau, E. Neher, Patch-clamp techniques for time-resolved capacitance measurements in single cells, Pflugers Arch. 411 (1988) 137–146.
[38] D. Oliver, B. Fakler, Expression density and functional characteristics of the outer hair cell motor protein are regulated during postnatal development in rat, J. Physiol. 519 (pt3) (1999) 791–800.

[39] M. Howarth, K. Takao, Y. Hayashi, A.Y. Ting, Targeting quantum dots to surface proteins in living cells with biotin ligase, Proc. Natl. Acad. Sci. USA 102 (2005) 7583–7588.
[40] G.J. Mize, J.E. Harris, T.K. Takayama, J.D. Kulman, Regulated expression of active biotinylated G-protein coupled receptors in mammalian cells, Protein Expr. Purif. 57 (2008) 280–289.
[41] J. Zheng, K.B. Long, W. Shen, L.D. Madison, P. Dallos, Prestin topology: localization of protein epitopes in relation to the plasma membrane, Neuroreport 12 (2001) 1929–1935.
[42] O.E. Okoruwa, M.D. Weston, D.C. Sanjeevi, A.R. Millemon, B. Fritzsch, R. Hallworth, K.W. Beisel, Evolutionary insights into the unique electromotility motor of mammalian outer hair cells, Evol. Dev. 10 (2008) 300–315.
[43] J. Santos-Sacchi, Reversible inhibition of voltage-dependent outer hair cell motility and capacitance, J. Neurosci. 11 (1991) 3096–3110.
[44] J.F. Ashmore, Forward and reverse transduction in the mammalian cochlea, Neurosci. Res. Suppl. 12 (1990) S39–S50.
[45] C. Solsona, B. Innocenti, J.M. Fernandez, Regulation of exocytotic fusion by cell inflation, Biophys. J. 74 (1998) 1061–1073.
[46] P. Dallos, B. Fakler, Prestin: a new type of motor protein, Nat. Rev. Mol. Cell Biol. 3 (2002) 104–111.
[47] G. Patterson, R.N. Day, D. Piston, Fluorescent protein spectra, J. Cell Sci. 114 (2001) 837–838.
[48] N. Panchuk-Voloshina, R.P. Haugland, J. Bishop-Stewart, M.K. Bhalgat, P.J. Millard, F. Mao, W.Y. Leung, Alexa dyes: a series of new fluorescent dyes that yield exceptionally bright, photostable conjugates, J. Histochem. Cytochem. 47 (1999) 1179–1188.